



K O N I N K L I J K E N E D E R L A N D S E
A K A D E M I E V A N W E T E N S C H A P P E N

On-site blackwater treatment fosters microbial groups and functions to efficiently and robustly recover carbon and nutrients

Kuramae, Eiko; Dimitrov, M.; Silva, G.H.R.; Lucheta, A.; Mendes, Lukas W.; Luz, Ronildson Lima; Vet, L.E.M.; Fernandes, T.V.

published in

Microorganisms
2021

DOI (link to publisher)

[10.3390/microorganisms9010075](https://doi.org/10.3390/microorganisms9010075)

document version

specify

document license

CC BY

[Link to publication in KNAW Research Portal](#)

citation for published version (APA)

Kuramae, E., Dimitrov, M., Silva, G. H. R., Lucheta, A., Mendes, L. W., Luz, R. L., Vet, L. E. M., & Fernandes, T. V. (2021). On-site blackwater treatment fosters microbial groups and functions to efficiently and robustly recover carbon and nutrients. *Microorganisms*, 9, [75]. <https://doi.org/10.3390/microorganisms9010075>

General rights

Copyright and moral rights for the publications made accessible in the public portal are retained by the authors and/or other copyright owners and it is a condition of accessing publications that users recognise and abide by the legal requirements associated with these rights.

- Users may download and print one copy of any publication from the KNAW public portal for the purpose of private study or research.
- You may not further distribute the material or use it for any profit-making activity or commercial gain.
- You may freely distribute the URL identifying the publication in the KNAW public portal.

Take down policy

If you believe that this document breaches copyright please contact us providing details, and we will remove access to the work immediately and investigate your claim.

E-mail address:

pure@knaw.nl

On-Site Blackwater Treatment Fosters Microbial Groups and Functions to Efficiently and Robustly Recover Carbon and Nutrients

Eiko E. Kuramae (✉ E.Kuramae@nioo.knaw.nl)

Netherlands Institute of Ecology (NIOO-KNAW) <https://orcid.org/0000-0001-6701-8668>

Mauricio R. Dimitrov

Nederlands Instituut voor Ecologie

Gustavo R.H. Silva

Universidade Estadual Paulista Julio de Mesquita Filho

Adriano Lucheta

Nederlands Instituut voor Ecologie

Lucas W. Mendes

Nederlands Instituut voor Ecologie

Ronildson L. Luz

Nederlands Instituut voor Ecologie

Louise Vet

Nederlands Instituut voor Ecologie

Tania V. Fernandes

Nederlands Instituut voor Ecologie

Research

Keywords: Blackwater microbiome, Phosphorus, Nitrogen, Chlorella sorokiniana, shotgun metagenomics

DOI: <https://doi.org/10.21203/rs.3.rs-60534/v1>

License:  This work is licensed under a Creative Commons Attribution 4.0 International License.

[Read Full License](#)

Abstract

Background: Wastewater is considered as a renewable resource water and energy. An advantage of decentralized sanitation systems is the separation of the blackwater (BW) stream, which is highly contaminated with human pathogens, from the remaining household water. However, the composition and functions of the microbial community in BW are not known. In this study, we used shotgun metagenomics to assess the dynamics of microbial community structure and function throughout a new BW anaerobic digestion system installed at The Netherlands Institute of Ecology. Samples from the influent (BW), primary effluent (anaerobic digested BW), sludge and final effluent of the pilot upflow anaerobic sludge blanket (UASB) reactor and microalgae pilot tubular photobioreactor (PBR) were analyzed.

Results: Our results showed a decrease in microbial richness and diversity followed by a decrease in functional complexity and co-occurrence along the different modules of the bioreactor. The microbial diversity and function decrease were reflected both changes in substrate composition and wash conditions. The most prevalent core functions in influent (BW) were related to metabolism of carbohydrates, response to chemicals and drugs, and nitrogen. The core functions in anaerobic digested BW and upflow anaerobic sludge blanket reactor were related to response to stress, viral processes and iron-sulfur metabolism. Methanogenesis-related functions were most abundant in upflow anaerobic sludge blanket reactor. Effluent from tubular photobioreactor presented high abundances of functions related to nitrogen utilization, metal ion binding and antibiotic biosynthetic processes. Interestingly, the abundance of sequences related to 'pathogenesis' decreased from influent BW to SP1 to effluent from tubular photobioreactor. Our wastewater treatment system also decreased potential microbial functions related to pathogenesis.

Conclusions: The new sanitation system studied here fosters microbial groups and functions that allow the system to efficiently and robustly recover carbon and nutrients while reducing pathogenic groups, ultimately generating a final effluent safe for discharge and reuse.

1. Background

The global demand for freshwater is rising at a rate of approximately 1% per year due to population growth, changes in consumption patterns, and economic development [1]. This increased demand comes as freshwater availability is decreasing due to climate change, unsustainable ground water consumption and other human activities [2]. Due to this unsustainable impact on the global water cycle, a growing number of people are living under conditions of water scarcity and reduced water quality, endangering aquatic ecosystems and public health [1]. Poor surface water and groundwater quality are due largely to a lack of wastewater treatment. According to a recent UN report, 80% of all wastewater (domestic and industrial) is discharged without treatment, resulting in physical, chemical and biological pollution [1]. Consequently, improving sanitation by increasing access to wastewater treatment is a priority in the UN's Sustainable Development Goals (SDG 6) as a recognized human right that is essential for food security,

health promotion and poverty reduction [3, 4]. Wastewater treatment can be applied in a centralized or decentralized manner. While the former requires a sewer connection, the latter can be applied on-site. Decentralized sanitation systems are increasingly deployed globally and can provide wastewater reuse, energy and nutrient recovery. New sanitation concepts that separate blackwater (BW – toilet wastewater containing feces, urine, toilet paper and flush water) and greywater (GW – shower/washing wastewater) at the source for treatment on-site conserve organic and inorganic compounds in a smaller volume, thus facilitating recovery [5].

In decentralized sanitation systems, the BW tank is a rich nutrient environment containing 82% of the total nitrogen and 68% of the total phosphorus present in domestic wastewater [6]. This environment also features several microbial communities that play an important role in wastewater treatment [7]. However, despite the development of this technology over the last 100 years, the associated microbial composition and functions remain unclear [7]. In BW tanks, microorganisms such as the anammox group are responsible for the biological and catalytic processes involved in nitrogen removal (anaerobic ammonium oxidation), while bacteria from the *Ureibacillus* genus can degrade organic matter [8, 9]. Based on 16S rRNA gene analyses, these processes are associated with different microbes (nitrite oxidation bacteria) that express functional genes (copper-containing nitrite reductase, nitrous oxide reductase, sulfate reductase) enabling the removal of toxins, contaminants and some nutrients [7, 10]. In addition, several studies have reported that decentralized systems efficiently reduce pathogens, including bacteria (*Salmonella* and *E. coli*) [11], protozoans (*Giardia* spp.) [12], helminths (*Ascaris lumbricoides*) [13], hookworms (*Strongyloides stercoralis*) and trophozoites (*Trichomonas* and *Enterobius vermicularis*) [11]. Therefore, adequate wastewater treatment systems that produce safe treated wastewater for reuse and resources, whether centralized or decentralized, are crucial for further recovery, reuse and recycling.

The Netherlands Institute of Ecology (NIOO-KNAW) in The Netherlands has implemented such a new decentralized sanitation system in its approximately 250-person office/laboratory building. The BW is vacuum-collected using only 1 L of ground water per flush and then treated in a UASB (upflow anaerobic sludge blanket) reactor, where the carbon is converted into biogas, a renewable energy source. Anaerobic treatment of concentrated BW is a proven technology for treating high-strength wastewater [5]. The remaining effluent, known as anaerobically treated BW (AnBW), contains the major part of the nutrients and is treated in a microalgae pilot tubular photobioreactor (PBR) (Fig. 1). After harvesting the microalgal biomass, the effluent is polished in a constructed wetland and finally discharged into surface water. By implementing a biological wastewater treatment strategy mimicking natural processes, we strive to achieve an efficient and robust process for wastewater reuse, carbon and nutrient recovery and a healthy final effluent that is safe to discharge. However, the microbiome composition in this system is unknown. Therefore, in this study, we assessed the dynamics of the microbial community structure and functions in this on-site BW digestion system by monitoring the influent (BW), primary effluent (anaerobic digested BW), sludge and finally the effluent of the UASB reactor and microalgae PBR. We hypothesize that the diversity of microbial community composition and function decrease along the different modules of the BW bioreactor due to changes in substrate composition.

2. Results

2.1. Physicochemical composition of the blackwater anaerobic digestion system

Table 1 shows the characteristics of the BW (SP1), sludge from the UASB reactor (SP-S), anaerobic digested blackwater (SP2) and effluent from the tubular PBR (SP3) used in this study. The sewage temperature varied between 15.2 and 33.5 °C during the entire study. The total chemical oxygen (COD_{total}), total nitrogen (TN), and total phosphorus (TP) varied between 11.3 and 22.7, 0.66 and 5.18, and 0.16 and 0.26 g.L⁻¹, respectively. The maximum removal of TN and TP in the UASB reactor was 44% and 53%, respectively. The COD_{total} in the effluent of the tubular PBR increased due to growth of the microalgae. During the experimental period, DO was low in SP1, SP-S and SP2, indicating anaerobic conditions. By contrast, due to photosynthetic oxygen evolution by the microalgae, an increase in the DO concentration was observed in the culture medium in SP3.

Table 1

Characteristics of the blackwater system in different treatment modules: blackwater (SP1), sludge from the UASB reactor (SP-S), anaerobic digested blackwater (SP2) and effluent from the tubular PBR (SP3).

Points of sampling	COD _{total} (g.L ⁻¹)	TN (g.L ⁻¹)	TP (g.L ⁻¹)	Alkalinity (g.L ⁻¹)	pH	TSS (g.L ⁻¹)	VSS (g.L ⁻¹)	T (°C)	OD mg.L ⁻¹
Average ± standard variation									
SP1	17.0 ± 4.7	2.53 ± 1.89	0.20 ± 0.05	4.85 ± 1.14	8.40 ± 0.30	8.2 ± 3.1	7.5 ± 3.1	18.0 ± 1.8	0.58 ± 1.02
SP-S	43.7 ± 3.4	3.85 ± 1.49	0.46 ± 0.08	5.19 ± 0.10	7.60 ± 0.40	45.8 ± 0.9	36.0 ± 1.2	21.6 ± 6.3	0.36 ± 0.57
SP2	6.7 ± 2.8	1.76 ± 1.26	0.14 ± 0.02	5.19 ± 0.10	7.70 ± 0.10	4.8 ± 2.4	4.6 ± 2.2	23.3 ± 9.3	0.63 ± 0.71
SP3	5.2 ± 2.6	1.42 ± 1.21	0.07 ± 0.01	0.44 ± 0.21	6.60 ± 0.40	2.8 ± 0.4	2.5 ± 0.1	22.0 ± 2.6	1.10 ± 0.62

COD_{total}=total chemical oxygen demand; TSS = total solids suspended, VSS = volatile solids suspended.

2.2. Microbial community structure

To visualize the differences in community structure among the treatments, taxonomic and functional abundance matrices were used for canonical correlation analysis (CCA) (Fig. 2). For taxonomy, the samples were grouped according to the treatment module (PERMANOVA F = 16.62, P < 0.0001), with no

differences between sampling times (Fig. 2A). For the functional profile, the same pattern of grouping was observed (PERMANOVA $F = 2.75$, $P = 0.031$), with no differences between sampling times (Fig. 2B). For both the taxonomy and functional profiles, the samples clustered in three main clusters: one for SP1, one for SP3 and one for SP2 together with SP-S (Fig. 2A, 2B).

2.3. Microbial community diversity and composition

Approximately 48,000 sequences of acceptable quality were generated and used for downstream analysis. The species richness did not differ significantly between the treatment modules, but a decreasing trend from SP1 to SP3 was observed (Fig. 3A). By contrast, a decrease in diversity was observed in SP3 (Fig. 3A). Comparing the effect of sampling time within each treatment module revealed increased diversity from times T0 to T2 (Additional file 1: Supplementary Figure S1). The majority of the 16S rRNA gene sequences were affiliated with bacteria (65% of all sequences), followed by 1% with archaea. The remaining 34% of the sequences could not be affiliated and were removed from further analysis. Interestingly, the proportions of bacterial and archaeal sequences differed among the treatment modules, with higher proportions of archaea in SP2 and SP-S (Additional file 1: Supplementary Figure S2). The phylum Bacteroidetes dominated the samples, with an average of 30% of all sequences, followed by Firmicutes (27.6%), Proteobacteria (15%), Cyanobacteria (11.74%), and Spirochaetes (3.7%). Of the 51 total phyla affiliated with our sequences, 23 presented significant variation in abundance among the treatment modules (Fig. 4A). SP1 hosted higher abundances of Bacteroidetes and Firmicutes, while SP3 presented higher abundances of Acidobacteria, Cyanobacteria, and Proteobacteria compared with the other treatment modules. SP2 and SP-S exhibited the most distinct environments, with 17 microbial phyla with higher abundances compared with SP1 and SP3, most notably Verrucomicrobia, Synergistetes, and two archaeal phyla. At a lower taxonomic level, the three most abundant genera were *Bacteroides*, *Prevotella*, and *Faecalibacterium* in SP1; *Bacteroides*, *Sphaerochaeta*, and *Treponema* in SP2; *Candidatus Cloacamonas*, *Clostridium*, and *Methanosaeta* in SP-S; and *Leptolyngbya*, *Acutodesmus*, and *Bacteroides* in SP3. In addition, the nitrifiers *Nitrosomonadaceae* and *Nitrobacter* were abundant only in SP3 (Additional file 1: Supplementary Figure S3).

2.4. Microbial functional profile

The functional profiles of different treatment modules were annotated using Gene Ontology database and compared using STAMP. The functional diversity did not differ among the treatment modules, but the richness of functions was higher in SP3 (Fig. 3B). Sampling time did not affect the overall functional diversity and richness (Additional file 1: Supplementary Figure S4).

In general, functions related to biological properties decreased from SP1 to SP3, functions related to cellular components were lower in SP1 and increased in the other treatments, and molecular functions were higher in SP1 and SP3 (Additional file 1: Supplementary Figure S5). A heatmap of selected functions that differed among the treatments is shown in Fig. 4B (for a complete list of functions, see Additional file 1: Supplementary Table S1). The most prevalent core functions in SP1 were related to metabolism of carbohydrates, response to chemicals and drugs, and nitrogen. The core functions in SP2

and SP-S were related to response to stress, viral processes and iron-sulfur metabolism. Methanogenesis-related functions were most abundant in SP-S. SP3 presented high abundances of functions related to nitrogen utilization, metal ion binding and antibiotic biosynthetic processes. Interestingly, the abundance of sequences related to 'pathogenesis' decreased from SP1 to SP3.

2.5. Co-occurrence network analysis

To explore the complexity and dynamics of the microbial communities in each treatment module, we conducted a co-occurrence network analysis by calculating SparCC correlations between microbial taxa at the genus level based on the 16S rRNA data. We further calculated the topological properties of the obtained networks to identify differences between the treatment modules. The network analyses showed that community complexity decreased from SP1 to SP3 (Fig. 5 and Table 2). SP1 was the most complex (89 nodes; 1081 edges; 7 community hubs; average degree of 24.29), followed by SP2 (37 nodes; 95 edges; 7 community hubs; av. degree of 5.13), SP3 (38 nodes; 86 edges; 6 hubs; av. degree of 4.52), and finally SP-S, the least complex (29 nodes; 51 edges; 6 hubs; av. degree of 3.51).

Table 2
Correlations and topological properties of the microbiome networks.

Network properties	SP1	SP2	SP-S	SP3
Number of nodes ^a	89	37	29	38
Number of edges ^b	1081	95	51	86
Positive edges ^c	1079	91	50	86
Negative edges ^d	2	4	1	0
Modularity ^e	0.139	0.384	0.352	0.364
Number of communities ^f	7	7	6	6
Network diameter ^g	6	6	5	8
Average path length ^h	2.019	2.494	2.602	2.842
Average degree ⁱ	24.29	5.13	3.517	4.52
Av. clustering coefficient ^j	0.741	0.573	0.445	0.469

^aMicrobial taxon (at genus level) with at least one significant ($P < 0.01$) and strong (SparCC > 0.7 or < -0.7) correlation;

^bNumber of connections/correlations obtained by SparCC analysis;

^cSparCC positive correlation (> 0.7 with $P < 0.01$);

^dSparCC negative correlation (< -0.7 with $P < 0.01$);

^eThe capability of the nodes to form highly connected communities, that is, a structure with high density of between nodes connections (inferred by Gephi);

^fA community is defined as a group of nodes densely connected internally (Gephi);

^gThe longest distance between nodes in the network, measured in number of edges (Gephi);

^hAverage network distance between all pair of nodes or the average length off all edges in the network (Gephi);

ⁱThe average number of connections per node in the network, that is, the node connectivity (Gephi);

^jHow nodes are embedded in their neighborhood and the degree to which they tend to cluster together (Gephi).

3. Discussion

The average $\text{COD}_{\text{total}}$, TN, and TP in the concentrated BW were 17.0, 2.53 and 0.20 g.L^{-1} , respectively. The concentration of $\text{COD}_{\text{total}}$ in the BW in the present study is higher than that reported by Zeeman et al. [5] and De Graaff et al. [42] for BW collected from vacuum toilets, but the concentrations of TN and TP are similar. The pH of the UASB reactor effluent was 7.70, within the recommended range for methanogenesis according to Chernicharo [14]. Alkalinity was higher in the effluent of the UASB reactor than in the influent, which is desirable because high concentrations of volatile acids can be buffered without causing a substantial drop in pH [14]. Appropriate total alkalinity can maintain the buffering capacity of the reactor at favorable levels [15]. The average $\text{COD}_{\text{total}}$ removal in the UASB reactor was 60.6%, lower than the value reported by De Graaff et al. (2010) due to some periods of instability in the influent flow of the reactor. The average removal of TN and TP in the UASB reactor was 30.4 and 30.0%, respectively; the majority of TN and TP remained in the liquid phase for subsequent removal/recovery in the tubular PBR. The TSS concentration in the sludge of the UASB reactor was 45.8 g.L^{-1} , which is classified as dense and flocculent according to Chernicharo (2017). The $\text{COD}_{\text{total}}$ in the effluent of the tubular PBR increased because of microalgal growth. The removal/recovery of TN and TP was 44.0% and 65.0%, respectively, from the influent to the tubular PBR.

Our results showed that the BW module increased microbial richness and diversity. From a microbial perspective, BW offers a wider niche for the UASB reactor, which likely promoted increased microbial community diversity via organic matter concentration. However, along the different modules of the bioreactor, the abundance of DNA sequences decreased dramatically. Also, the network analysis showed a decrease in the microbial community complexity from the beginning to the final steps of the bioreactor

(SP1 to SP3), concomitant to a reduced diversity. Such a decrease is reasonable and reflects both changes in substrate composition and wash conditions. In the initial stage, the BW promoted increases in Bacteroidetes, Firmicutes, and Proteobacteria, which accounted for more than 60% of all DNA sequences affiliated to bacteria. Previous studies have reported the presence and high abundance of Bacteroidetes in human feces and water environments [16–18]. Bacteroidetes play an important role in acidification in UASB sludge [16, 18]. Moreover, Bacteroidetes are a group of proteolytic bacteria with a robust capacity to decompose proteins, amino acids, and high-molecular-weight compounds in water environments, explaining the dominance of this phylum in the initial phase [19, 20].

The high abundance and strong shifts in the phyla Bacteroidetes, Firmicutes, and Proteobacteria dominated the composition of the common microbiome in the BW module [21]. This is because Bacteroidetes and Firmicutes are capable of degrade various types of cellulose, mainly from toilet paper [18]. In the initial phase at BW there is a large amount of cellulose biomass which contributed to select cellulose-degrading bacteria. The high abundance of cellulose-degrading bacteria found in our study play an important role on fiber decomposition. The fiber decomposition compound can accumulate and hazardous impact the other steps such as sludge production and biogas production during the anaerobic processes [22]. Moreover, the predominance of Firmicutes in the SP1 tanks indicate a dependence on molecules produced by other groups of microorganisms once these syntrophic bacteria are capable of degrading cellulosic compounds and producing volatile fatty acids (VFAs) and H_2 , which are then consumed by hydrogenotrophic methanogens in metabolic reactions [23]. The third most abundant phylum, Proteobacteria, predominated in the SP3 tanks. This phylum comprises sulfate-reducing groups of bacteria that, like Firmicutes, are syntrophic and depends on symbioses (associated with methanogens) [24].

We also found significantly higher abundances of Acidobacteria and Cyanobacteria in the SP3 tanks. Members of the phylum Cyanobacteria are able to thrive in several critical conditions in bioreactor tanks. According to Stal [25], Cyanobacteria oxidize sulfides under anoxic conditions and perform anoxygenic photosynthesis utilizing a hydrogen sulfide-like electron donor. In a study of biofilms containing Cyanobacteria in scum from a bioreactor, [26] observed spatial proximity between Cyanobacteria and hydrogen sulfide bacteria.

The microbial community also showed several different functions along the bioreactor. The SP1 tank promoted functions related to the metabolism of carbohydrates, chemicals, drugs, and nitrogen. Human waste sewage is composed mainly of high concentrations of nitrogen and carbohydrates [27, 28]. Organic nitrogen is the major nitrogen form in human feces. Therefore, the transformation of organic nitrogen to its inorganic forms (ammonia/ammonium) requires an association with bacterial groups such as Bacteroidetes and Firmicutes [29][30]. Those groups likely transformed the nitrogen in the bioreactor system since they were the most abundant groups in the first stage of water decontamination. Bacteroidetes and Firmicutes also degrade carbohydrates in the human gut [31][32], their original habitat before transitioning to the bioreactor. In SP1, we also identified other functions related to cellular components such as stimulus, molecule transport, and pathogenesis. All these functions are likely

associated with the high diversity of fecal components, which stimulates cell activity in the initial phase of the bioreactor.

In SP-S, we detected nitrogen metabolic processes resulting from initial nitrogen transformation. We also detected several other functions related to the exchange of electron acceptors and anaerobic transformation of waste. The syntrophic groups *Synergistetes*, *Parvachaeota*, and *Chloroflexi* play important roles in anaerobic processes [10, 33, 34]. According to [33], the predominance of these methanogenic groups indicates a syntrophic relationship with other bacterial groups. In the present study we also found high correlation with methanogenesis process in the SP-S. This function is directly related to the methanogenic degradation of toilet paper [35]. The water insoluble cellulose from toilet paper are a significant fraction of sewage and although cellulose is a type of carbohydrate its decomposition is very slow [36]. We here found that the partial degraded cellulose by Bacteroidetes and Firmicutes from SP1 activated the methanogenesis process from methanogenic *Chloroflexi* and *Synergistetes* at the SP-S which converted cellulose in methane.

In SP3, we found a high abundance of functions related to regulation of nitrogen, antibiotic biosynthetic and metal ion binding. Those functions are related to microalgal activity, which has shown efficient performance in decontaminating water [37–39]. In addition, these same microalgae have been shown to be used as rich nutrient in barley production [40]. Our system of wastewater treatment also decreased microbial functions related to pathogenesis, and the analyses confirmed that the microalgae-containing SP3 reduced bacterial richness and diversity. Consistent with our findings, [41] reported high performance of an algae system in reducing pathogenic bacteria.

4. Conclusions

In summary, the new pilot sanitation system developed at the Netherlands Institute of Ecology fosters microbial groups and functions that enable an efficient and robust process for carbon and nutrient recovery and apparently reduce potential pathogenic groups, resulting in a healthy final effluent that is much safer for discharge.

5. Materials And Methods

5.1. Blackwater samples

BW was collected for the experiments from vacuum toilets (1 L of water/flush) at the NIOO-KNAW building (Fig. 1) in Wageningen, the Netherlands (SP1). The BW consists only of feces, urine, toilet paper and approximately one liter of ground water. Anaerobic treatment of BW has proved to be the core technology for nutrient and energy recovery [6, 42]. At NIOO, a UASB reactor operating at 35 °C is installed to treat the BW (SP2). The reactor has a volume of 893 L and is designed based on a hydraulic residence time (HRT) of 8.7 days. The diameter and height of the UASB reactor are 0.66 m and 2.75 m, respectively, with 5 taps installed every 0.46 m from the bottom to monitor the sludge bed (SP-S – first tap from the

bottom). The effluent of the UASB reactor was treated in a pilot-scale tubular PBR inoculated with the microalgal species *Chlorella sorokiniana* (SP3). The tubular PBR consists of two parallel systems that are connected to ensure homogeneous content. Each system consists of 25 m of horizontal tubes and two vertical air lift columns. At the top of the air lift columns, a cylindrical box ensures complete mixing of the tubular PBR's content. The inner diameter of the horizontal tubes is 5.6 cm, and the inner diameter of the air lift columns is 12 cm. The horizontal tubes, airlift columns and top box have volumes of 140 L, 63 L, and 8 L, respectively, resulting in a total volume of approximately 211 L. Wastewater samples were collected from the BW (SP1), sludge from the UASB reactor (SP-S), anaerobic digested BW (SP2), and effluent from the tubular PBR (SP3) three times ($t = 0$, $t = 1$ and $t = 2$) with one week between each sampling time (Fig. 1). Collected samples were homogenized and sub-samples were taken to perform chemical and microbial analysis. The sub-samples for microbial community analysis were immediately frozen with liquid nitrogen at the sampling moment and stored until DNA extraction. Temperature, pH and dissolved oxygen were measured during sampling with field meters.

5.2. Chemical analysis

Total nitrogen (TN), total phosphorus (TP), total chemical oxygen demand ($\text{COD}_{\text{total}}$), total suspended solids (TSS), volatile suspended solids (VSS), dissolved oxygen (DO) and alkalinity were all measured according to standard methods at the chemical laboratory of the Netherlands Institute of Ecology, Wageningen.

5.3. DNA extraction

Samples were collected from four points of the sanitation system as described above and illustrated in Fig. 1: SP1, SP-S, SP2 and SP3. For each sample, three biological replicates were obtained. The total DNA of each sample replicate was extracted from 250 mg of material using the PowerSoil® DNA Isolation Kit (MO BIO Laboratories, Inc.) according to the manufacturer's instructions. The extracted DNA was quantified by a spectrophotometer (NanoDrop™ 2000, Thermo Fisher Scientific, Massachusetts, USA) and visualized by 1.0% agarose gel electrophoresis and ethidium bromide staining. The total DNA was used for metagenome shotgun sequencing. Library preparation and Illumina HiSeq XTen sequencing were performed at BGI Genomics, China. The resulting sequences were deposited in the European Nucleotide Archive (ENA; <https://www.ebi.ac.uk/ena>) under accession number PRJEB19684.

5.4. DNA shotgun metagenome analyses

The sequence data were processed using EBI pipeline version 3 (<https://www.ebi.ac.uk/metagenomics/pipelines/3.0>) for classification into different functional categories. Then, the classified function sequences were classified according to taxonomy using Kaiju <http://kaiju.binf.ku.dk> [43]. The potential functions and taxonomy of the microbial communities in the different treatments were analyzed as described in the Statistical analysis section.

5.5. Statistical analysis

To compare the taxonomic and functional microbial structures and determine their correlations with chemical factors among the treatments, we performed canonical correspondence analysis (CCA). For this, the matrices were initially analyzed using detrended correspondence analysis (DCA) to evaluate the gradient size of the species distribution, which indicated a non-linear distributed data (length of gradient > 4), revealing that the best-fit mathematical model for the data was CCA. Forward selection (FS) and Monte Carlo permutation tests were applied with 1,000 random permutations to verify the significance of the physicochemical properties for the microbial community. To test whether the sample categories harbored significantly different microbial community structures, we performed permutational multivariate analysis of variance (PERMANOVA) [44]. Alpha diversity was calculated from a matrix of richness at the species level using Shannon's index. CCA plots were generated using Canoco 4.5 software (Biometrics, Wageningen, The Netherlands), and PERMANOVA and alpha diversity indexes were calculated with the software PAST 3 (Hammer et al., 2001). To visualize differences in microbial community composition among the treatments, we generated taxonomic and functional matrices as input for the software Statistical Analysis of Metagenome Profile (STAMP) [45]. The comparison was based on P-values calculated using the two-sided Welch's t-test, and correction was performed using the Benjamini-Hochberg false discovery rate [46]. For visualization, heatmaps were constructed based on the z-score-transformed phylum/function abundances to improve the normality and homogeneity of the variances.

In addition, network analyses were performed to assess the dynamics of the interactions among the microbial communities in each module: SP1, SP-S, SP2, and SP3. Non-random co-occurrence analyses were performed using SparCC, a tool capable of estimating correlation values from compositional data [47]. We calculated SparCC correlations between microbial taxa at the genus level based on the metagenome taxonomic affiliation. For each network analysis, *P*-values were obtained by 99 permutations of random selections of the data table, subjected to the same analytical pipeline. SparCC correlations with a magnitude > 0.7 or < -0.7 and statistical significance ($P < 0.01$) were included in the network analyses. The nodes in the reconstructed networks represent OTUs at the genus level, whereas the edges (that is, connections) correspond to strong and significant correlations between nodes. The topology of the network was calculated based on a set of measures, including the numbers of nodes and edges, modularity, number of communities, average path length, network diameter, average degree and clustering coefficient ([48, 49]. Co-occurrence analyses were carried out using the Python module 'SparCC' and network visualization, and properties measurements were calculated with the interactive platform Gephi (Bastian et al., 2009).

Declarations

Funding

This research was supported by The Netherlands Organization for Scientific Research (NWO) under grant number 729.004.003; São Paulo Research Foundation (FAPESP) under grant number 2013/50351-4; Brazilian National Council for Scientific and Technological Development (CNPq) under grant number 206884/2014-1. Publication number XXXX of The Netherlands Institute of Ecology (NIOO-KNAW).

Availability of data and materials

The sequences were deposited in the European Nucleotide Archive (ENA; <https://www.ebi.ac.uk/ena>) under accession number PRJEB19684.

Authors' contributions

E.E.K: Conceptualization, Writing & editing - original draft, Funding acquisition, Writing – review and editing, Supervision. M.D.: Metagenome analysis, Bioinformatics. G.H.R.S.: run the experiment, chemical data analysis, Writing. A.L.: Sampling for DNA extraction, DNA extraction. L.W.M.: data analysis. R.L.L.: Investigation. L.V.: Funding acquisition. T.V.F.: Resources, Writing – review. All authors reviewed the manuscript.

Ethics approval and consent to participate

Not applicable.

Competing interests

The authors declare that they have no competing interests.

Acknowledgements

We thank Rebeca Arias and Agata Pijl for laboratory assistance and Minh Trần Triết for the illustration of Fig. 1.

References

1. Water U. UN World Water Development Report, Nature-based Solutions for Water. 2018.
2. Rodell M, Famiglietti JS, Wiese DN, Reager JT, Beaudoing HK, Landerer FW, et al. Emerging trends in global freshwater availability. *Nature*. 2018;557:651–9.
3. Ait-Kadi M. Water for Development and Development for Water: Realizing the Sustainable Development Goals (SDGs) Vision. *Aquatic Procedia*. 2016;6:106–10.
4. Molle F, Mollinga P. Water poverty indicators: conceptual problems and policy issues. *Water Policy*. 2003;5:529–44.
5. Zeeman G, Kujawa K, Mes TZD de, Graaff MS de, Abu-Ghunmi LNAH, Mels AR, et al. Anaerobic treatment as a core technology for energy, nutrients and water from source-separated domestic waste(water). *Water Sci Technol*. 2008;57:1207–12.
6. Kujawa-Roeleveld K, Zeeman G. Anaerobic Treatment in Decentralised and Source-Separation-Based Sanitation Concepts. *Reviews in Environmental Science Bio/Technology*. 2006;5:115–39.
7. Shu D, He Y, Yue H, Wang Q. Microbial structures and community functions of anaerobic sludge in six full-scale wastewater treatment plants as revealed by 454 high-throughput pyrosequencing.

- Biores Technol. 2015;186:163–72.
8. Nakasaki K, Tran LTH, Idemoto Y, Abe M, Rollon AP. Comparison of organic matter degradation and microbial community during thermophilic composting of two different types of anaerobic sludge. *Biores Technol.* 2009;100:676–82.
 9. van Kessel MA, Stultiens K, Slegers MF, Guerrero Cruz S, Jetten MS, Kartal B, et al. Current perspectives on the application of N-damo and anammox in wastewater treatment. *Curr Opin Biotechnol.* 2018;50:222–7.
 10. Wang H, Zeng Y, Guo C, Bao Y, Lu G, Reinfelder JR, et al. Bacterial, archaeal, and fungal community responses to acid mine drainage-laden pollution in a rice paddy soil ecosystem. *Science of The Total Environment.* 2018;616–617:107–16.
 11. Samhan SA, Al-Sa'ed RM, Mahmoud NJ. Removal of pathogenic microorganisms in pilot-scale UASB-septic tanks and Albireh urban wastewater treatment plant in Palestine. *Water Int.* 2007;32:798–809.
 12. Medeiros RC, Daniel LA, de Oliveira GL, Hoffmann MT. Performance of a small-scale wastewater treatment plant for removal of pathogenic protozoa (oo)cysts and indicator microorganisms. *Environ Technol.* 2019;40:3492–501.
 13. Zhang L, De Vrieze J, Hendrickx TLG, Wei W, Temmink H, Rijnaarts H, et al. Anaerobic treatment of raw domestic wastewater in a UASB-digester at 10 °C and microbial community dynamics. *Chem Eng J.* 2018;334:2088–97.
 14. Chernicharo CAL, Brandt EMF, Bressani-Ribeiro T, Melo VR, Bianchetti FJ, MotaFilho CR, et al. Development of a tool for improving the management of gaseous emissions in UASB-based sewage treatment plants. *Water Practice Technology.* 2017;12:917–26.
 15. Sánchez E, Borja R, Travieso L, Martín A, Colmenarejo MF. Effect of organic loading rate on the stability, operational parameters and performance of a secondary upflow anaerobic sludge bed reactor treating piggery waste. *Biores Technol.* 2005;96:335–44.
 16. Lu X, Ni J, Zhen G, Kubota K, Li Y-Y. Response of morphology and microbial community structure of granules to influent COD/SO₄²⁻ – ratios in an upflow anaerobic sludge blanket (UASB) reactor treating starch wastewater. *Biores Technol.* 2018;256:456–65.
 17. Ozgun H, Gimenez JB, Ersahin ME, Tao Y, Spanjers H, van Lier JB. Impact of membrane addition for effluent extraction on the performance and sludge characteristics of upflow anaerobic sludge blanket reactors treating municipal wastewater. *J Membr Sci.* 2015;479:95–104.
 18. Syutsubo K, Yoochatchaval W, Tsushima I, Araki N, Kubota K, Onodera T, et al. Evaluation of sludge properties in a pilot-scale UASB reactor for sewage treatment in a temperate region. *Water Sci Technol.* 2011;64:1959–66.
 19. Fernández-Gómez B, Richter M, Schüller M, Pinhassi J, Acinas SG, González JM, et al. Ecology of marine Bacteroidetes: a comparative genomics approach. *The ISME Journal.* 2013;7:1026–37.
 20. Rivière D, Desvignes V, Pelletier E, Chaussonnerie S, Guermazi S, Weissenbach J, et al. Towards the definition of a core of microorganisms involved in anaerobic digestion of sludge. *The ISME Journal.*

- 2009;3:700–14.
21. Cardinali-Rezende J, Araújo JC, Almeida PGS, Chernicharo CAL, Sanz JL, Chartone-Souza E, et al. Organic loading rate and food-to-microorganism ratio shape prokaryotic diversity in a demo-scale up-flow anaerobic sludge blanket reactor treating domestic wastewater. *Antonie Van Leeuwenhoek*. 2013;104:993–1003.
 22. Li S, Wu Z, Liu G. Degradation kinetics of toilet paper fiber during wastewater treatment: Effects of solid retention time and microbial community. *Chemosphere*. 2019;225:915–26.
 23. Hattori S, Kamagata Y, Hanada S, Shoun H. *Thermacetogenium phaeum* gen. nov., sp. nov., a strictly anaerobic, thermophilic, syntrophic acetate-oxidizing bacterium. *Int J Syst Evol Microbiol*. 2000;50:1601–9.
 24. Guerrero L, Omil F, Méndez R, Lema JM. Anaerobic hydrolysis and acidogenesis of wastewaters from food industries with high content of organic solids and protein. *Water Res*. 1999;33:3281–90.
 25. STAL LJ. Physiological ecology of cyanobacteria in microbial mats and other communities. *New Phytol*. 1995;131:1–32.
 26. Garcia GP, Souza CL, Glória RM, Silva SQ, Chernicharo CAL. Biological oxidation of sulphides by microorganisms present in the scum layer of UASB reactors treating domestic wastewater. *Water Sci Technol*. 2012;66:1871–8.
 27. Li Q, Wang XC, Zhang HH, Shi HL, Hu T, Ngo HH. Characteristics of nitrogen transformation and microbial community in an aerobic composting reactor under two typical temperatures. *Biores Technol*. 2013;137:270–7.
 28. Zoetendal EG, Raes J, van den Bogert B, Arumugam M, Booiijink CC, Troost FJ, et al. The human small intestinal microbiota is driven by rapid uptake and conversion of simple carbohydrates. *The ISME Journal*. 2012;6:1415–26.
 29. Cobo-Díaz JF, Fernández-González AJ, Villadas PJ, Robles AB, Toro N, Fernández-López M. Metagenomic Assessment of the Potential Microbial Nitrogen Pathways in the Rhizosphere of a Mediterranean Forest After a Wildfire. *Microb Ecol*. 2015;69:895–904.
 30. Inoue J, Oshima K, Suda W, Sakamoto M, Iino T, Noda S, et al. Distribution and Evolution of Nitrogen Fixation Genes in the Phylum Bacteroidetes. *Microbes Environments*. 2015;30:44–50.
 31. Flint HJ, Scott KP, Duncan SH, Louis P, Forano E. Microbial degradation of complex carbohydrates in the gut. *Gut Microbes*. 2012;3:289–306.
 32. Rios-Covian D, Salazar N, Gueimonde M, de los Reyes-Gavilan CG. Shaping the Metabolism of Intestinal Bacteroides Population through Diet to Improve Human Health. *Front Microbiol*. 2017;8:376.
 33. Jang HM, Kim JH, Ha JH, Park JM. Bacterial and methanogenic archaeal communities during the single-stage anaerobic digestion of high-strength food wastewater. *Biores Technol*. 2014;165:174–82.
 34. Yamada T, Sekiguchi Y, Imachi H, Kamagata Y, Ohashi A, Harada H. Diversity, Localization, and Physiological Properties of Filamentous Microbes Belonging to *Chloroflexi* Subphylum

- I in Mesophilic and Thermophilic Methanogenic Sludge Granules. *Appl Environ Microbiol.* 2005;71:7493.
35. Chen R, Nie Y, Kato H, Wu J, Utashiro T, Lu J, et al. Methanogenic degradation of toilet-paper cellulose upon sewage treatment in an anaerobic membrane bioreactor at room temperature. *Biores Technol.* 2017;228:69–76.
 36. Ruiken CJ, Breuer G, Klaversma E, Santiago T, van Loosdrecht MCM. Sieving wastewater – Cellulose recovery, economic and energy evaluation. *Water Res.* 2013;47:43–8.
 37. Di Termini I. On the nitrogen and phosphorus removal in algal photobioreactors. *Ecological engineering.* 2011;37:976–80.
 38. Gao F, Li C, Yang Z-H, Zeng G-M, Mu J, Liu M, et al. Removal of nutrients, organic matter, and metal from domestic secondary effluent through microalgae cultivation in a membrane photobioreactor. *Journal of Chemical Technology Biotechnology.* 2016;91:2713–9.
 39. Shi X, Yeap TS, Huang S, Chen J, Ng HY. Pretreatment of saline antibiotic wastewater using marine microalga. *Biores Technol.* 2018;258:240–6.
 40. Suleiman AKA, Lourenço KS, Clark C, Luz RL, da Silva GHR, Vet LEM, et al. From toilet to agriculture: Fertilization with microalgal biomass from wastewater impacts the soil and rhizosphere active microbiomes, greenhouse gas emissions and plant growth. *Resources, Conservation and Recycling.* 2020;161:104924.
 41. Delanka-Pedige HMK. Pathogen reduction in an algal-based wastewater treatment system employing *Galdieria sulphuraria*. *Algal research.* 2019;2019.
 42. De Graaff MS, Temmink H, Zeeman G, Buisman CJN. Anaerobic Treatment of Concentrated Black Water in a UASB Reactor at a Short HRT. *Water.* 2010;2.
 43. Menzel P, Ng KL, Krogh A. Fast and sensitive taxonomic classification for metagenomics with Kaiju. *Nat Commun.* 2016;7:11257.
 44. Anderson MJ. A new method for non-parametric multivariate analysis of variance. *Austral Ecol.* 2001;26:32–46.
 45. Parks DH, Tyson GW, Hugenholtz P, Beiko RG. STAMP: statistical analysis of taxonomic and functional profiles. *Bioinformatics.* 2014;30:3123–4.
 46. Benjamini Y, Hochberg Y. Controlling the False Discovery Rate: A Practical and Powerful Approach to Multiple Testing. *Journal of the Royal Statistical Society Series B (Methodological).* 1995;57:289–300.
 47. Friedman J, Alm EJ. Inferring Correlation Networks from Genomic Survey Data. *PLOS Computational Biology.* 2012;8:e1002687.
 48. Newman MEJ. Modularity and community structure in networks. *Proc Natl Acad Sci USA.* 2006;103:8577.
 49. Newman MEJ. The structure and function of networks. *Comput Phys Commun.* 2002;147:40–5.

Figures

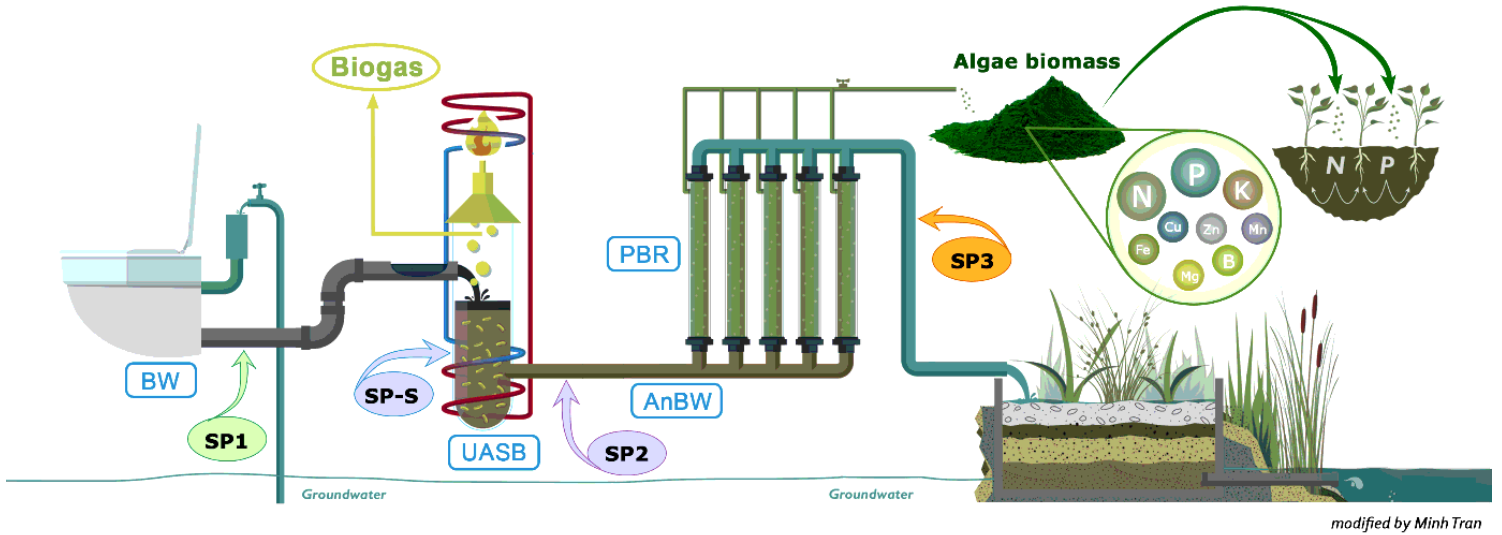


Figure 1

On-site black water treatment scheme at NIOO-KNAW used for the evaluation of the microbial communities in different treatment modules: blackwater (SP1), sludge from the UASB reactor (SP-S), anaerobic digested blackwater (SP2) and effluent from the tubular PBR (SP3).

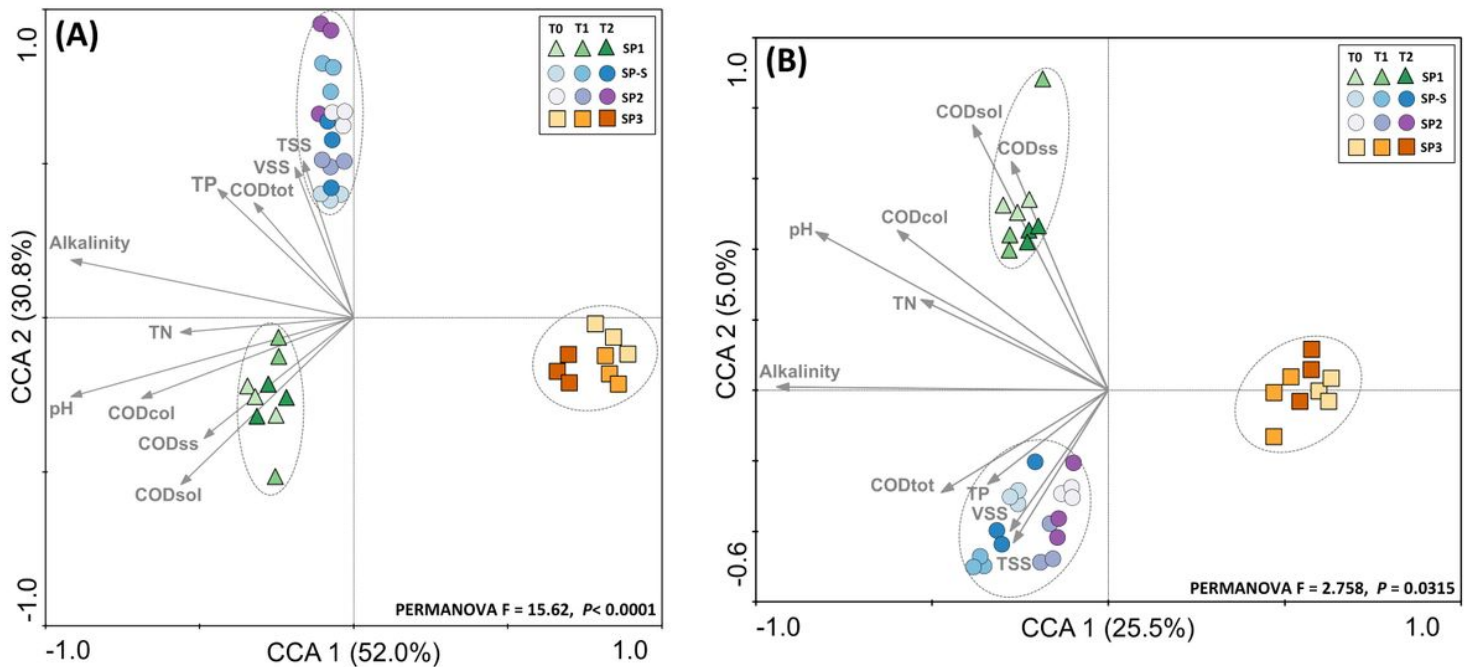


Figure 2

Canonical correspondence analysis (CCA) of the (A) taxonomic and (B) functional profiles and correlation with the physicochemical characteristics of on-site blackwater treatment. The arrows indicate the

correlations between the physicochemical parameters and microbial profiles. Significant clusters (PERMANOVA, $P < 0.05$) are indicated by dashed lines in the graph.

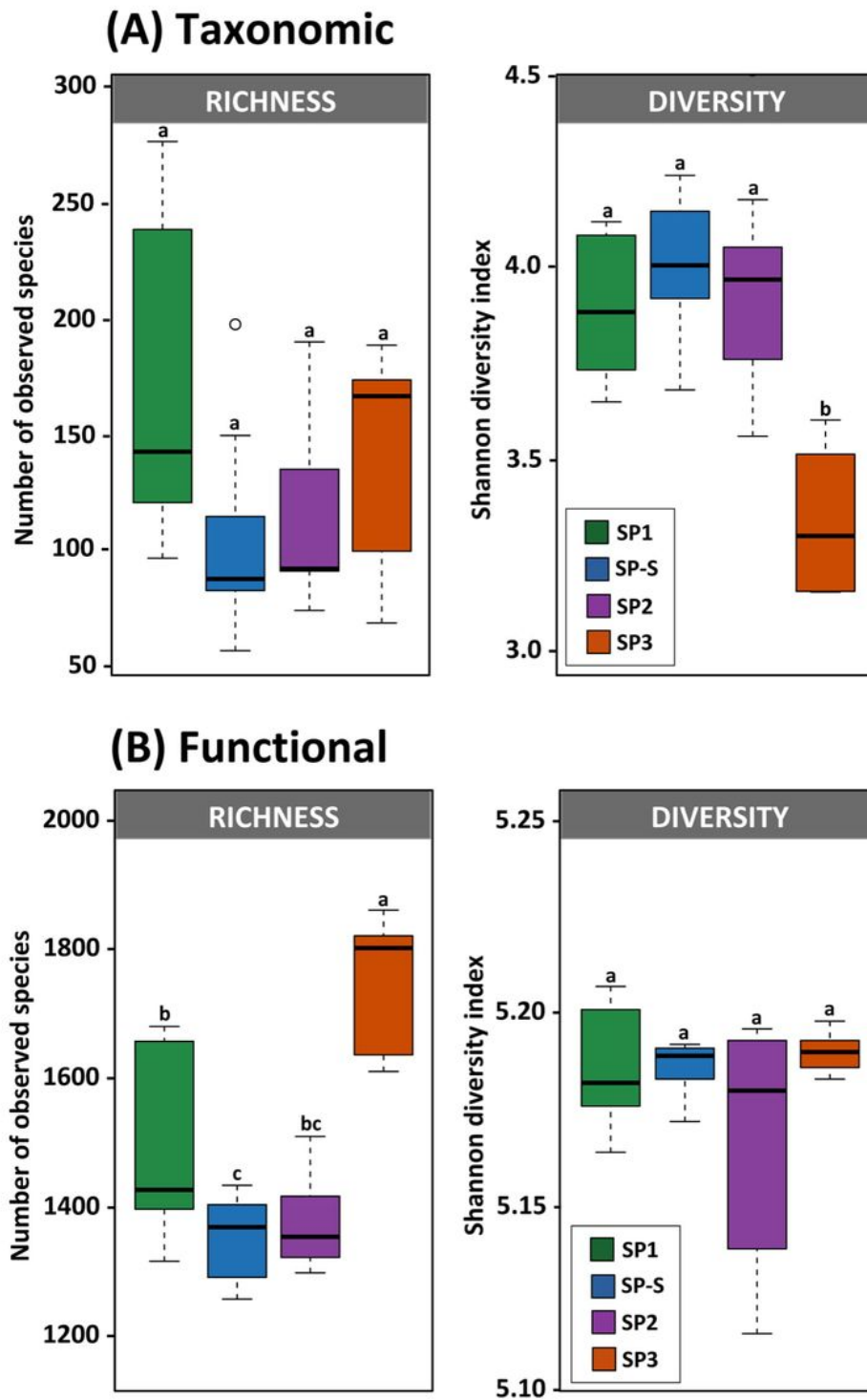


Figure 3

Diversity measurements of (A) taxonomic and (B) functional profiles based on DNA shotgun metagenome analysis. Different lowercase letters refer to significant differences between treatments based on Tukey's HSD test ($P < 0.05$).

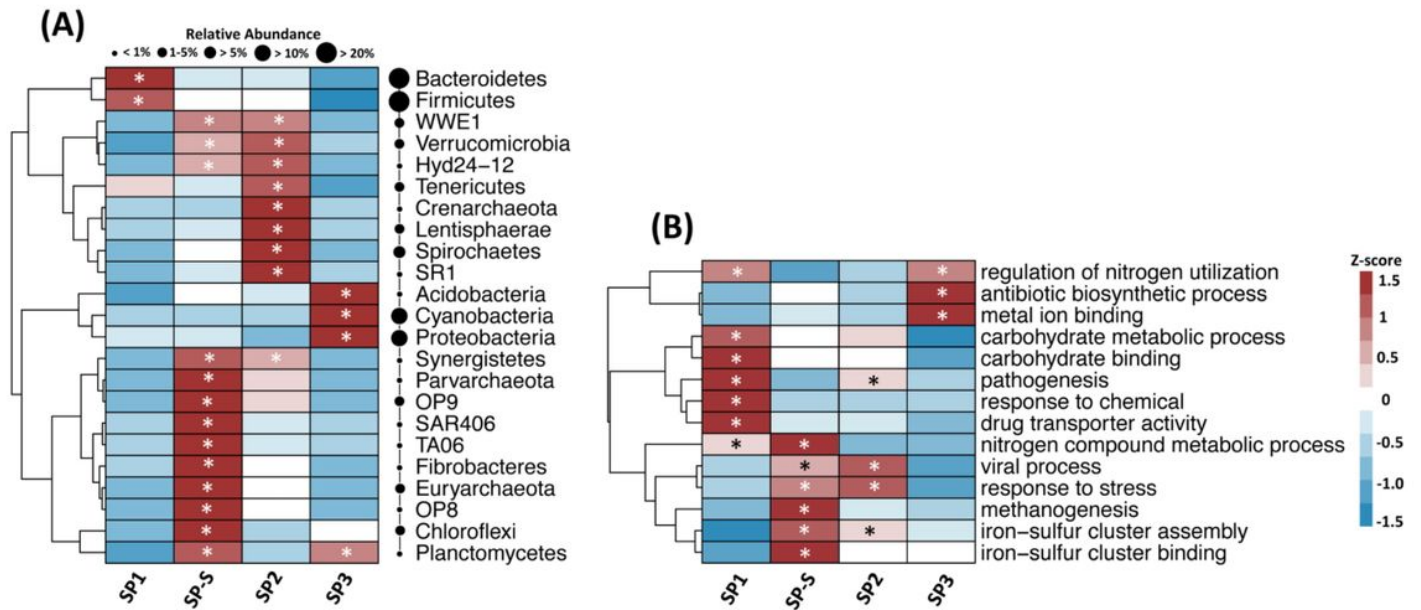


Figure 4

Heatmaps showing the differential abundance of (A) bacterial phyla and (B) functional categories in the on-site blackwater treatment system. The color key relates the heatmap colors to the standard score (z-score), i.e., the deviation from the row mean in units of standard deviation above or below the mean. Asterisks indicate significantly different group abundances based on the two-sided Welch's t-test with Benjamini-Hochberg false discovery rate correction ($P < 0.05$). The circles are proportional to the relative abundance of each phylum in all samples. Only phyla with significant differences between treatment modules are included in the figure.

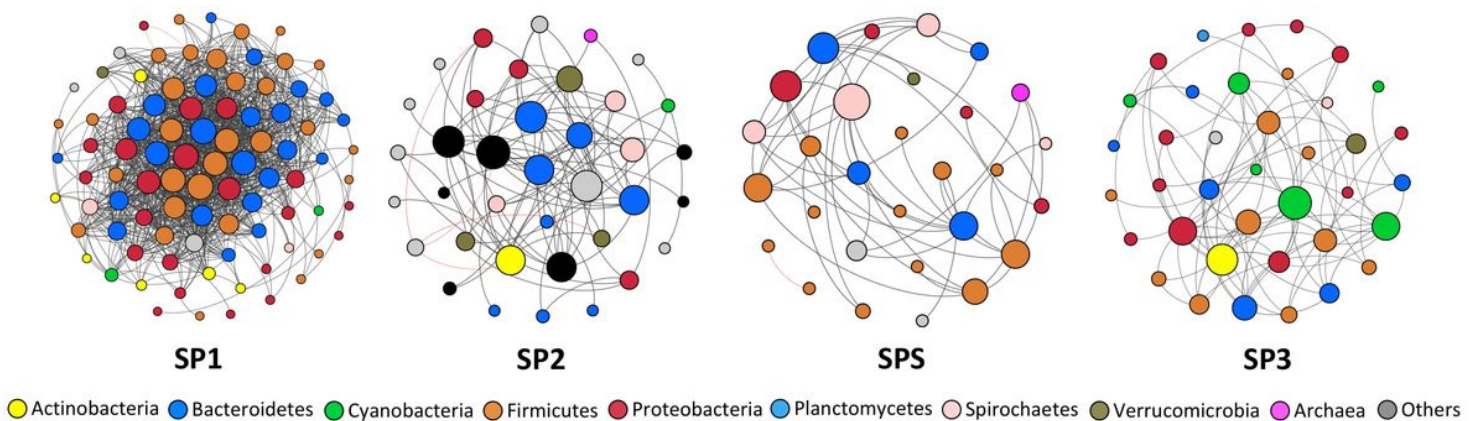


Figure 5

Network co-occurrence analysis of microbial communities from the on-site blackwater treatment system. A connection indicates a SparCC correlation with a magnitude of > 0.7 (positive correlation – black edges) or < -0.7 (negative correlation – red edges) and statistical significance ($P < 0.01$). Each node

represents a different bacterial genus, and the size of the node is proportional to the number of connections (degree). Each node is labelled at the phylum level.

Supplementary Files

This is a list of supplementary files associated with this preprint. Click to download.

- [SupplementaryMaterial.docx](#)